



Published in final edited form as:

Nat Med. 2012 June ; 18(6): 943–949. doi:10.1038/nm.2756.

NF- κ B-inducing kinase (NIK) promotes hyperglycemia and glucose intolerance in obesity by augmenting glucagon action

Liang Sheng¹, Yingjiang Zhou¹, Zheng Chen¹, Decheng Ren¹, Kae Won Cho¹, Lin Jiang¹, Hong Shen¹, Yoshiteru Sasaki², and Liangyou Rui^{1,*}

¹Department of Molecular & Integrative Physiology, University of Michigan Medical School, Ann Arbor, MI 48109, USA

²Laboratory for Stem Cell Biology, Riken Center for Developmental Biology, Kobe 650-0047, Japan

Abstract

The canonical IKK β /NF- κ B1 pathway has been well documented to promote insulin resistance; however, the noncanonical NIK/NF- κ B2 pathway is poorly understood in obesity. Additionally, the contribution of counterregulatory hormones, particularly glucagon, to hyperglycemia in obesity remains unclear. Here we show that NIK promotes glucagon responses in obesity. Hepatic NIK was abnormally-activated in mice with dietary or genetic obesity. Systemic deletion of NIK decreased glucagon responses and hepatic glucose production (HGP). Obesity is associated with increased glucagon responses, and liver-specific inhibition of NIK decreased glucagon responses and HGP and protected against hyperglycemia and glucose intolerance. Conversely, hepatocyte-specific overexpression of NIK increased glucagon responses and HGP. In isolated livers and primary hepatocytes, NIK also promoted glucagon action and glucose production, at least in part by increasing CREB stability. Therefore, overactivation of liver NIK in obesity promotes hyperglycemia and glucose intolerance by increasing the hyperglycemic response to glucagon and other factors that activate CREB.

Keywords

NIK; Obesity; glucagon; type 2 diabetes; gluconeogenesis; glucose counterregulation; CREB; inflammation

Obesity is associated with chronic inflammation which is believed to contribute to the pathogenesis of type 2 diabetes^{1,2}. Proinflammatory cytokines activate the canonical IKK β /NF- κ B1 and the JNK pathways, which is believed to impair glucose metabolism by

Users may view, print, copy, download and text and data- mine the content in such documents, for the purposes of academic research, subject always to the full Conditions of use: http://www.nature.com/authors/editorial_policies/license.html#terms

*Address Correspondence to: Liangyou Rui, Ph.D., Department of Molecular & Integrative Physiology, University of Michigan Medical School, Ann Arbor, MI 48109-0622, TEL: (734) 615-7544, FAX: (734) 647-9523, rui@umich.edu.

Disclosure Statement: All authors have nothing to declare.

Author Contributions

L.R. and L.S. designed the experiments and prepared the manuscript. L.S., Y.Z., Z.C., D.R., K.W.C., L.J., H.S. performed experiments. Y.S. generated STOP-NIK mice.

increasing insulin resistance³⁻⁵. Blood glucose is determined by a balance between insulin and counterregulatory hormones (e.g. glucagon, catecholamines, glucocorticoids, and growth hormone)⁶. In the fasting state, glucagon is secreted by pancreatic α cells and increases hepatic glucose production (HGP) by stimulating hepatic glycogenolysis and gluconeogenesis⁶. Glucagon stimulates phosphorylation and activation of CREB via the cAMP/protein kinase A pathway, and CREB in turn activates the transcription of key gluconeogenic enzymes, including phosphoenolpyruvate carboxykinase (PEPCK) and glucose-6-phosphatase (G6Pase)⁷. In rodents with type 1 diabetes, increased glucagon action appears to be a determinant factor for hyperglycemia and glucose intolerance⁸⁻¹⁰. Blood glucagon levels are elevated in rodents with insulin deficiency, and leptin treatments normalize hyperglucagonemia and hyperglycemia^{8,9}. Deletion of glucagon receptors prevents streptozotocin (STZ)-induced hyperglycemia and glucose intolerance¹⁰. In a type 2 diabetes model, leptin treatments also attenuate hyperglucagonemia, leading to improvement in hyperglycemia and glucose intolerance¹¹. Insulin suppresses glucagon secretion from α cells¹²; therefore, α cell insulin resistance may lead to hyperglucagonemia which contributes to hyperglycemia in type 2 diabetes.

A subset of cytokines also stimulate the noncanonical NF- κ B-inducing kinase (NIK)/NF- κ B2 pathway; however, the metabolic function of this pathway has not been examined. It is also unclear whether inflammation alters glucagon responses. NIK, also called MAP3K14 (accession number: NM_003954), is an essential upstream Ser/Thr kinase of the noncanonical NF- κ B2 pathway¹³. NIK protein levels are extremely low in quiescent cells due to rapid degradation, and cytokines or oxidative stress increases NIK protein stability, leading to NIK activation¹⁴. NIK has been reported to regulate B and T cell development in animals^{15,16}. In this study, we show that liver NIK is aberrantly activated in obesity and increases HGP by promoting glucagon action, thus contributing to hyperglycemia and glucose intolerance. NIK promotes glucagon action at least in part by increasing CREB stability.

RESULTS

NIK is abnormally activated in the livers of obese mice

We measured NIK activity in commonly-used mouse models of obesity: dietary obesity and genetic obesity with leptin-deficiency (*ob/ob*). NIK were immunopurified from the liver and subjected to *in vitro* kinase assays with glutathione-S transferase (GST)-IKK α (amino acids 108–368) fusion protein as substrate. GST-IKK α contains a NIK phosphorylation site (IKK α Ser176) and lacks catalytic activity¹⁷. NIK activity in the liver was 10-fold higher in *ob/ob* mice (13 wks) versus wild-type (WT) mice (Fig. 1a). Liver NIK activity was also 14-fold higher in mice fed a high fat diet (HFD) versus a normal chow diet (Fig. 1b). NIK protein was detected in *ob/ob* mice (Fig. 1a), but undetectable in WT mice due to rapid degradation^{18,19}. Levels of the active form (p52) of NF- κ B2 in the liver were higher in both *ob/ob* (versus WT) and HFD-fed (versus chow-fed) mice (Fig. 1c). In contrast, NIK activity in skeletal muscles was similar between lean and obese mice (Supplementary Fig. 1a).

Obesity is associated with chronic inflammation, oxidative stress, and steatosis in the liver^{1,2}. To determine whether these factors contribute to NIK activation, we examined the

ability of TNF- α (mimic inflammation), H₂O₂ (oxidative stress), and palmitic acid (PA) (steatosis) to stimulate NIK. Recombinant NIK was introduced into mouse primary hepatocytes via NIK adenoviral infection, and the cells were subsequently treated with these compounds. TNF- α , H₂O₂, or PA treatments increased both NIK autophosphorylation and the ability of NIK to phosphorylate GST-IKK α (Fig. 1d). TNF- α , H₂O₂, and PA also stimulated endogenous NIK in hepatocytes (Supplementary Fig. 1b).

Inhibition of liver NIK improves glucose metabolism in obese mice

To examine the metabolic function of NIK *in vivo*, we characterized previously-generated NIK knockout (KO) mice¹⁵. The active form of NF- κ B2 (p52) was abundant in WT but not KO hepatocytes (Supplementary Fig. 2a). TNF- α similarly stimulated I κ B degradation as well as phosphorylation of I κ B, p38, and JNK in both WT and KO hepatocytes (Supplementary Fig. 2b). These results verify the previous findings that NIK is required for the noncanonical, but not the canonical, NF- κ B pathways¹⁵. Notably, KO mice had hypoglycemia (Fig. 2a) and improved glucose tolerance compared with WT littermates (Fig. 2b). HGP, estimated by pyruvate tolerance tests (PTT), was lower in KO than WT mice (Fig. 2c). Plasma insulin levels (Supplementary Fig. 2c) and insulin tolerance (Fig. 2d) were relatively normal in KO mice.

To examine the role of liver NIK, NIK was selectively inhibited in the liver by overexpressing kinase-inactive NIK(KA) via tail vein injection of NIK(KA) adenoviruses. NIK(KA) contains substitutions of Lys^{429/430} with Ala and acts as a dominant negative mutant of NIK^{20,21}. Flag-tagged NIK(KA) was detected in the livers of NIK(KA), but not β -gal, adenovirus-infected mice and inhibited liver NIK activity (Fig. 2e). Mice were fed an HFD for 12 weeks and infected with NIK(KA) or β -gal adenoviruses. HFD promoted hyperglycemia; liver-specific inhibition of NIK significantly ameliorated HFD-induced hyperglycemia (Fig. 2f), hyperinsulinemia (Supplementary Fig. 3a), glucose intolerance (Fig. 2g), and insulin resistance (Fig. 2g). HGP, estimated by PTT, was also lower in NIK(KA) than in β -gal adenovirus-infected mice (Fig. 2g). Body weight and liver size were similar between the NIK(KA) and the β -gal groups (Supplementary Fig. 3b,c). In *db/db* (lacking functional leptin receptors) mice, blood glucose was inversely correlated with NIK(KA) expression. NIK(KA) was detected in the liver 13 days after NIK(KA) adenoviral infection and undetectable 53 days after infection (Fig. 2h). Blood glucose decreased to the lowest levels 10–20 days after NIK(KA) adenoviral infection, and then increased progressively to reach levels similar to that of the β -gal group 40 days after infection (Fig. 2h). Glucose intolerance (Fig. 2i), insulin resistance (Fig. 2i), and hyperinsulinemia (Supplementary Fig. 3d) were also significantly improved in the NIK(KA) group versus the β -gal group. Body weight and liver TNF- α expression were similar between the NIK(KA) and β -gal groups (Supplementary Fig. 3e,f). In *ob/ob* mice, liver-specific overexpression of NIK(KA) also reduced hyperglycemia (Supplementary Fig. 3g), glucose intolerance (Supplementary Fig. 3h), insulin resistance (Supplementary Fig. 3i), and HGP (Supplementary Fig. 3j). To further study NIK in hepatocytes, we generated STOP-NIK(KA) adenoviruses (Fig. 3a). NIK(KA) expression was blocked by a STOP cassette and was able to be reactivated by Cre-mediated excision of the STOP cassette. To verify hepatocyte-specific expression of NIK(KA), WT and albumin-Cre^{+/-} mice were infected

with STOP-NIK(KA) or β -gal adenoviruses. NIK(KA) was detected in the livers of albumin-Cre^{+/-} but not WT mice (Fig. 3b). Albumin-Cre^{+/-} mice were fed an HFD and infected with STOP-NIK(KA) or green fluorescent protein (GFP) adenoviruses. Blood glucose (Fig. 3c), glucose intolerance (Fig. 3d), and HGP (Fig. 3e) were significantly lower in the STOP-NIK(KA) versus the GFP groups. In contrast, STOP-NIK(KA) adenoviral infection neither decreased blood glucose nor improved glucose intolerance in WT mice (data not shown). Taken together, these data indicate that liver-specific inhibition of NIK decreases hyperglycemia and glucose intolerance in both dietary and genetic obesity independently of body weight changes.

To determine whether activation of liver NIK is sufficient to alter glucose metabolism, we generated mice with hepatocyte-specific overexpression of Flag-tagged NIK (Hep^{NIK}) using previously-generated STOP-NIK mice²². In STOP-NIK mice, a *STOP-NIK* transgene was knocked in the *Rosa26* locus (Fig. 3f), and the STOP cassette blocked the expression of Flag-tagged NIK (Fig. 3g, lane 1). STOP-NIK mice were crossed with albumin-Cre mice to generate Hep^{NIK} mice (genotype: *STOP-NIK*^{+/-}/*Cre*^{+/-}). In Hep^{NIK} mice, Cre-mediated excision of the STOP sequences was restricted to hepatocytes, resulting in modest expression of Flag-tagged NIK in the liver but not pancreas, muscle, brain, white fat, brown fat, spleen, kidney, and heart (Fig. 3g). Glucose tolerance and pyruvate tolerance were impaired in Hep^{NIK} males (fed a normal chow diet) compared with STOP-NIK (Hep^{CON}) mice (genotype: *STOP-NIK*^{+/-}/*Cre*^{-/-}) (Fig. 3h,i). Hep^{NIK} females (fed an HFD) also developed hyperglycemia and glucose intolerance (Supplementary Fig. 4a,b).

NIK promotes HGP by enhancing glucagon action

To directly measure HGP, livers were isolated and subjected to ex vivo gluconeogenesis assays. In WT mice, hepatic gluconeogenesis was 1.4-fold higher in the fasting state versus the fed state (Fig. 4a). Fasting-stimulated gluconeogenesis was 92% lesser in KO than in WT livers (Fig. 4a). Deletion of NIK also inhibited glucose production in primary hepatocytes under both basal and DB-cAMP/dexamethasone-stimulated conditions (Fig. 4b). Deletion of NIK decreased both the expression of hepatic G6Pase (by 80%) and PEPCK (by 75%) and the catalytic activity of G6Pase (by 48%) (Fig. 4c). NIK(KA)-mediated, liver-specific inhibition of NIK also suppressed the expression of hepatic PEPCK and G6Pase in *db/db* mice (Fig. 4d). Conversely, hepatocyte-specific overexpression of NIK increased G6Pase expression in both males (Fig. 4e) and females (Supplementary Fig. 4c).

To gain insights into the mechanism of NIK action, we examined insulin signaling. Deletion of NIK did not enhance insulin-stimulated phosphorylation of Akt (Fig. 4f) and FOXO1 (Supplementary Fig. 4d). Overexpression of NIK or NIK(KA) did not impair insulin-stimulated phosphorylation of Akt (Fig. 4g) and IRS1 (Supplementary Fig. 4e). In mice with STZ-induced insulin-deficiency, NIK(KA)-mediated, liver-specific inhibition of NIK still improved hyperglycemia and glucose intolerance (Fig. 4h). Therefore, insulin is less likely to mediate NIK regulation of HGP.

Glucagon appears to be responsible for hyperglycemia and glucose intolerance in STZ-treated animals^{9,10}, so we examined glucagon responses in NIK null mice. The hyperglycemic response to glucagon was significantly lower in KO than in WT littermates

(Fig. 4i), and KO mice had compensatory hyperglucagonemia (Fig. 4j). Glucagon resistance in KO mice was reversed by liver-specific reconstitution of recombinant NIK (Supplementary Fig. 4f). Hepatocyte-specific overexpression of NIK enhanced glucagon responses in Hep^{NIK} versus Hep^{CON} mice (Fig. 4j). In primary hepatocytes, NIK enhanced, whereas NIK(KA) impaired, glucagon-stimulated glucose production (Supplementary Fig. 5). In contrast, overexpression of kinase-inactive, dominant negative IKK β (KA) did not alter basal and glucagon-stimulated glucose production (Supplementary Fig. 5). Therefore, NIK enhances glucagon stimulation of HGP independently of IKK β .

NIK mediates increased glucagon action in obesity

To examine glucagon responses in obesity, we performed glucagon tolerance tests in WT mice fed an HFD for 6 weeks. Blood glucose levels were significantly higher at each time point after glucagon injection in mice fed an HFD than in mice fed a chow diet (Fig. 5a). Glucagon-stimulated increase in blood glucose was larger in HFD-fed than in chow diet-fed mice (Fig. 5b). Liver-specific inhibition of NIK significantly decreased glucagon responses in NIK(KA) adenovirus-infected mice versus β -gal adenovirus-infected mice (Fig. 5c).

Obesity is associated with liver inflammation, oxidative stress, and steatosis. To determine whether these factors enhance glucagon action, primary hepatocytes were pretreated with TNF- α , H₂O₂, and PA prior to glucagon stimulation. TNF- α , H₂O₂, and PA significantly increased both basal and glucagon-stimulated glucose production in WT hepatocytes (Fig. 5d). Deletion of NIK greatly attenuated the ability of TNF- α , H₂O₂, and PA to enhance glucagon responses in KO versus WT hepatocytes (Fig. 5d,e). TNF- α , H₂O₂, and PA treatments significantly increased glucagon-stimulated expression of PEPCK and G6Pase in WT hepatocytes (Fig. 5f). Deletion of NIK largely blocked the effect of TNF- α , H₂O₂, and PA in KO hepatocytes (Fig. 5g).

NIK phosphorylates CREB and increases CREB stability

CREB mediates glucagon stimulation of gluconeogenesis^{23–27}. CREB protein levels in both the liver and purified hepatocytes were lower in KO than in WT littermates (Fig. 6a). CREB phosphorylation (pSer¹³³) was also lower in KO than in WT mice (Fig. 6a). Liver-specific restoration of CREB reversed glucagon resistance in KO mice (Supplementary Fig. 6). Conversely, liver CREB was higher in Hep^{NIK} than in Hep^{CON} mice (Fig. 6b). Liver CREB levels were also higher in mice with either dietary (HFD versus chow diets) or genetic obesity (*ob/ob* versus WT) (Fig. 6c); in agreement, liver NIK activity was abnormally high in these obese mice (Fig. 1). Notably, hepatic CREB mRNA levels were similar between KO and WT mice (Supplementary Fig. 7a,b) and between Hep^{CON} and Hep^{NIK} mice (Supplementary Fig. 7c).

We hypothesized that NIK increases CREB protein stability. To test this idea, we introduced Flag-tagged CREB into primary hepatocytes with β -gal, NIK, or NIK(KA) via adenoviral infection. CREB mRNA levels were similar between β -gal, NIK, and NIK(KA) adenovirus-infected cells (Supplementary Fig. 7d); however, CREB protein levels were higher in NIK-expressing and lower in NIK(KA)-expressing cells versus that in β -gal-expressing cells (Supplementary Fig. 7e). To determine whether proteasomes is involved in CREB

degradation, KO and WT hepatocytes were infected with CREB adenoviruses and treated with MG132, a proteasome inhibitor. CREB levels were lower in KO than in WT cells, and MG132 markedly increased recombinant CREB in KO cells (Fig. 6d). MG132 also increased endogenous CREB in KO hepatocytes (Fig. 6e). In agreement, CREB ubiquitination was higher in KO than in WT hepatocytes (Supplementary Fig. 7f).

To determine whether NIK phosphorylates CREB, we performed *in vitro* kinase assays using immunopurified CREB, NIK, and NIK(KA). CREB was robustly phosphorylated by NIK but not NIK(KA) (Fig. 6f). Ser¹¹⁴ and Ser¹⁴² were identified as phosphorylation sites in NIK-overexpressing hepatocytes, using LC/MS/MS proteomics approaches. However, NIK still phosphorylated a CREB mutant lacking Ser¹¹¹, Ser¹¹⁴, and Ser¹⁴² sites (Supplementary Fig. 8a). We replaced Ser^{98,108,111,114,117,121,129,142,143,156,271,340}/Thr¹⁰⁰ (13 known sites) with Ala in CREB (13S-A). 13S-A was unable to be phosphorylated by NIK (Fig. 6g). To determine whether these sites are involved in NIK regulation of CREB stability, we introduced CREB or 13S-A into HepG2 cells expressing low levels of recombinant NIK. 13S-A migrated slightly faster than CREB in SDS-PAGE gels; NIK increased CREB, but not 13S-A, protein abundance (Fig. 6h). However, NIK at high levels increased the amount of both CREB and 13S-A proteins (Supplementary Fig. 8b,c). NIK at low levels increased 2S-A (Ser^{117,121} to Ala, Ser^{114,117} to Ala, or Ser^{114,121} to Ala) (Supplementary Fig. 8d), but not 3S-A (Ser^{114,117,121} to Ala) and 4S-A (Ser^{111, 114, 117, 121} to Ala) protein abundance (Fig. 6i). In contrast, NIK at high levels increased 3S-A protein abundance (Supplementary Fig. 8e). Therefore, NIK is able to increase CREB stability by both phosphorylation-dependent and -independent mechanisms.

DISCUSSION

We have identified NIK overactivation in the liver as a contributing factor to hyperglycemia and glucose intolerance in obesity. NIK was aberrantly activated in the livers of mice with either dietary or genetic obesity. Systemic deletion of NIK decreased blood glucose and improved glucose tolerance. In both dietary and genetic obesity, liver-specific inhibition of NIK markedly improved hyperglycemia and glucose intolerance. In agreement, hepatocyte-specific overexpression of NIK is sufficient to promote glucose intolerance.

We have discovered a new function of NIK in liver glucose metabolism. NIK promotes HGP by enhancing the hyperglycemic response to glucagon, a key counterregulatory hormone. In animals, deletion of NIK resulted in a reduction in HGP, glucagon resistance, and compensatory hyperglucagonemia. Similarly, liver-specific inhibition of NIK also decreased HGP and impaired glucagon responses. Conversely, hepatocyte-specific overexpression of NIK increased HGP and glucagon responses. In isolated livers and/or primary hepatocytes, deletion of NIK decreased both basal and glucagon-stimulated HGP. At molecular levels, NIK phosphorylated CREB and increased CREB protein stability by both phosphorylation-dependent and -independent mechanisms. Deletion of NIK decreased, whereas NIK overexpression increased, the levels of hepatic CREB protein but not mRNA. CREB mediates glucagon-stimulated hepatic gluconeogenesis^{23–25}. Consistently, systemic deletion or liver-specific inhibition of NIK decreased, whereas hepatocyte-specific overexpression increased, the expression of gluconeogenic *PEPCK* and *G6Pase*, two CREB

targets. Therefore, NIK is a new positive regulator of hepatic gluconeogenesis by enhancing the action of glucagon and/or other factors that activate the PKA/CREB pathway. However, our data do not exclude the possibility that NIK may regulate glucose metabolism by other mechanisms in addition to increasing CREB stability and glucagon responses.

We showed that obesity is associated with elevated glucagon responses. Liver-specific inhibition of NIK decreased glucagon responses, suggesting that overactivation of liver NIK is the major contributor to abnormal glucagon responses in obesity. Notably, TNF- α , H₂O₂, and PA activated NIK in hepatocytes, suggesting that inflammation, oxidative stress, and/or steatosis contribute to NIK overactivation in obesity. Under normal conditions, NIK is recruited to cIAP1/2 E3 ligases by a TRAF3/TRAF2 complex, leading to ubiquitination and proteasome-mediated degradation of NIK^{28–30}. Cytokine stimulation promotes degradation of TRAF3, resulting in NIK stabilization and activation^{29,30}. In future studies, it is important to examine how inflammation, oxidative stress, and steatosis promote activation of hepatic NIK in obesity. We also observed that TNF- α , H₂O₂, and PA enhanced glucagon-stimulated glucose production and expression of gluconeogenic genes in a NIK-dependent manner in primary hepatocytes. These results suggest that hepatic inflammation, oxidative stress, and/or steatosis activate NIK that in turn promotes glucagon responses and HGP, thereby contributing to hyperglycemia and glucose intolerance in obesity.

In conclusion, we show that obesity is associated with the activation of the noncanonical NIK/NF- κ B2 pathway in addition to the canonical IKK β /NF- κ B1 pathway in the liver. The NIK pathway increases HGP by enhancing glucagon and/or other counterregulatory hormone responses, whereas the IKK β pathway promotes insulin resistance. Both elevated counterregulatory hormone responses and insulin resistance contribute to hyperglycemia and glucose intolerance in obesity. Thus, NIK may serve as a new therapeutic target for the treatment of type 2 diabetes.

Methods

Animals

ob/ob, *db/db*, Albumin-Cre, and WT mice (in C57BL/6 background) for HFD experiments were from the Jackson Laboratory. NIK KO and WT mice (in 129/Sv and C57BL/6 mixed background) were from Robert Schreiber (Washington University School of Medicine, St. Louis, MO). STOP-NIK mice (in C57BL/6 background) were from Klaus Rajewsky (Harvard Medical School, Boston, MA 02115). STOP-NIK mice were crossed with Albumin-Cre mice to generate Hep^{CON} and Hep^{NIK} mice (in C57BL/6 background). Mice were housed on a 12-h light and 12-h dark cycle in the Unit for Laboratory Animal Medicine at the University of Michigan (ULAM) and fed either a normal chow diet (9% fat; Lab Diet) or an HFD (45% fat; Research Diets) *ad libitum* with free access to water. Animal experiments were conducted following protocols approved by the University Committee on the Use and Care of Animals (UCUCA).

Glucose, pyruvate, insulin, and glucagon tolerance tests

Glucose (2 g kg⁻¹ body weight) and insulin (1 unit kg⁻¹ body weight) tolerance tests have been described previously³¹. For pyruvate tolerance tests, mice were fasted overnight and intraperitoneally injected with pyruvate (2 g kg⁻¹ body weight). For glucagon tolerance tests, mice were fasted for 5 h and intraperitoneally injected with glucagon (15 µg kg⁻¹ body weight). Blood glucose was monitored after injection. In a few experiments, a different dose of glucose, insulin or glucagon was used as described in the figure legends.

Immunoprecipitation, immunoblotting, G6Pase activity assays, adenoviral infection, and qPCR

Immunoprecipitation, immunoblotting, G6Pase activity, adenoviral infection, and qPCR methods have been described previously^{32–34}. Relative mRNA abundance of PEPCK, G6Pase, CREB, and TNF-α were measured by qPCR and normalized to mRNA levels of β-*actin*. qPCR primers were: PECK-F: 5'-ATCATCTTTGGTGGCCGTAG-3', PECK-R: 5'-ATCTTGCCCTTGTTCTGC-3'; G6Pase-F: 5'-CCGGTGTGTTGAACGTCATCT-3', G6Pase-R: 5'-CAATGCCTGACAAGACTCCA-3'; CREB-F: 5'-AAGCAGCACGGAAGAGAGAG-3', CREB-R: 5'-GGTTTTCAAGCACTGCCACT-3'; TNF-α-F: 5'-CATCTTCTCAAAATTCGAGTGACAA-3', TNF-α-R: 5'-TGGGAGTAGACAAGGTACAACCC-3'; β-actin-F: 5'-AAATCGTGCCTGACATCAAA-3', β-actin-R: 5'-AAGGAAGGCTGGAAAAGAGC-3'. We used antibody to the following proteins for immunoblotting: NIK (Santa Cruz, sc-7211; 1:2,000), Flag (Sigma, F1804; 1:10,000), tubulin (Santa Cruz, sc-5286; 1:4,000), NF-κB2 (Santa Cruz, sc-7386; 1:3,000), phospho-Akt (pSer473) (Cell Signaling, #9271; 1:5,000), phospho-Akt (pThr308) (Cell Signaling, #9275; 1:3,000), Akt1 (Santa Cruz, sc-1618; 1:8,000), CREB (Santa Cruz, sc-186; 1:3,000), phospho-CREB (pSer133) (Santa Cruz, sc-7978; 1:3,000), LaminB1 (Abcam, Ab16048; 1:1,000), Histone H4 (Santa Cruz, sc-10810; 1:1,000), IκBα (Cell Signaling, #4812; 1:1,000), phospho-IκBα (Cell Signaling, #2859; 1:1,000), phospho-p38 (Cell Signaling, #4631; 1:3,000), p38 (Santa Cruz, sc-7149; 1:3,000), phospho-JNK (Santa Cruz, sc-6254; 1:2,000), JNK (Cell Signaling, #9252; 1:2,000), phospho-FOXO1 (Santa Cruz, sc-101681; 1:1,000), FOXO1 (Cell Signaling, #2880; 1:2,000), and ubiquitin (Sigma, SAB4503053; 1:1,000).

Liver and hepatocyte glucose production assays

HGP was measured in perfused livers as previously described^{35–37}. Briefly, mouse livers were isolated and perfused at 37°C in an incubator sequentially with Krebs-Ringer bicarbonate (KRB) buffer (119 mM NaCl, 5 mM KCl, 2.6 mM KH₂PO₄, 2.6 mM MgSO₄, 2 mM CaCl₂, 24.6 mM NaHCO₃, 10 mM HEPES, pH 7.4) for 10 min, glycogenolysis buffer (KRB buffer supplemented with 3% mannitol) for 15 min, and gluconeogenesis buffer (glycogenolysis buffer supplemented with 5 mM lactate and 5 mM pyruvate) for 20 min. All perfusion buffers were continuously oxygenated with 95% O₂ and 5% CO₂. The glycogenolysis and gluconeogenesis perfusates were recycled. Glucose concentrations in perfusates were measured using Glucose LiquiColor kits (Fisher Scientific Inc.). Gluconeogenesis was calculated by subtracting glycogenolysis from HGP. Gluconeogenesis rates were normalized to liver weights.

Primary hepatocytes were grown in William's medium E (Sigma) supplemented with 2% FBS, 100 units ml⁻¹ penicillin, and 100 µg ml⁻¹ streptomycin, and infected with adenoviruses as described previously³⁴. For glucose production assays, growth medium was replaced with KRB buffer supplemented with 0.5% BSA and gluconeogenic substrates (10 mM lactate and 5 mM pyruvate) in the presence or absence of 50 nM glucagon (or 10 µM N6,2'-O-Dibutyryl adenosine 3',5'-cyclic monophosphate and 100 nM dexamethasone). Hepatocytes were incubated for 4 h at 37°C, and culture medium was collected and used to measure glucose levels. Glucose production was normalized to total hepatocyte protein levels. In a few experiments (Figure 5), hepatocytes were pretreated with a combination of TNF-α (10 ng ml⁻¹), H₂O₂ (100 nM), and PA (100 µM) for 4 h prior to glucose production assays.

In vitro kinase assays

NIK was immunopurified using antibody to NIK (endogenous NIK) or Flag (recombinant NIK) and incubated with γ-[³²P]-ATP (2 µCi) and GST-IKKα(108–368) fusion protein (0.5 µg) in a kinase buffer (20 mM HEPES, pH 7.5–7.6, 33 µM ATP, 10 mM MgCl₂, 50 mM NaCl, 1 mM DTT, 10 µg ml⁻¹ aprotinin, 10 µg ml⁻¹ leupeptin, 1 mM Na₃VO₄) at 30°C for 30 min. The reactions were stopped by adding SDA-PAGE loading buffer and boiling for 5 min. Proteins were resolved by SDS-PAGE, transferred onto nitrocellulose membrane, and visualized by autoradiography. The membranes were subsequently immunoblotted with antibodies against GST, NIK, or Flag. In a few experiments (Fig. 6g), Flag-tagged NIK was overexpressed in hepatocytes via adenoviral infection, and immunopurified with antibody to Flag. HEK293 cells were transfected with plasmids expressing Myc-tagged CREB or 13S-A; cell extracts were boiled for 3 min to inactivate kinases, and then immunoprecipitated with antibody to Myc. Immunopurified NIK was mixed with CREB or 13S-A and subjected to *in vitro* kinase assays.

Nuclear extract preparation

Liver tissues or hepatocytes were homogenized in a lysis buffer (20 mM HEPES, 1 mM EDTA, 250 mM Sucrose, 10 µg ml⁻¹ aprotinin, 10 µg ml⁻¹ leupeptin, 1 mM PMSF, 1 mM Na₃VO₃, 0.2 mM benzamide, 0.5 mM DTT, pH 7.4) and centrifuged sequentially at 1100×g and 4000×g (at 4°C). Pellets were resuspended in a high salt solution (20 mM HEPES, 420 mM NaCl, 0.2 mM EDTA, 0.5 mM DTT, 1 mM PMSF, 1 mM Na₃VO₃, pH 7.9), and protein concentrations were measured using Bio-Rad protein assay kits.

HepG2 cell Transfection

CREB and NIK plasmids (1.2 µg) were incubated with 12 µl polyethylenimine (1 mg ml⁻¹) in 100 µl serum-free DMEM for 15 min and added to HepG2 cell suspension (6×10⁵ cells in 0.5 ml serum-free DMEM). Cells were plated into 12-well plates, incubated at 37°C for 4 h, and then grown in DMEM supplemented with 8% FBS.

Statistical Analysis

Data were presented as means ± s.e.m. Differences between groups were analyzed with two-tailed Student's *t* test. *P* < 0.05 was considered statistically significant.

Supplementary Material

Refer to Web version on PubMed Central for supplementary material.

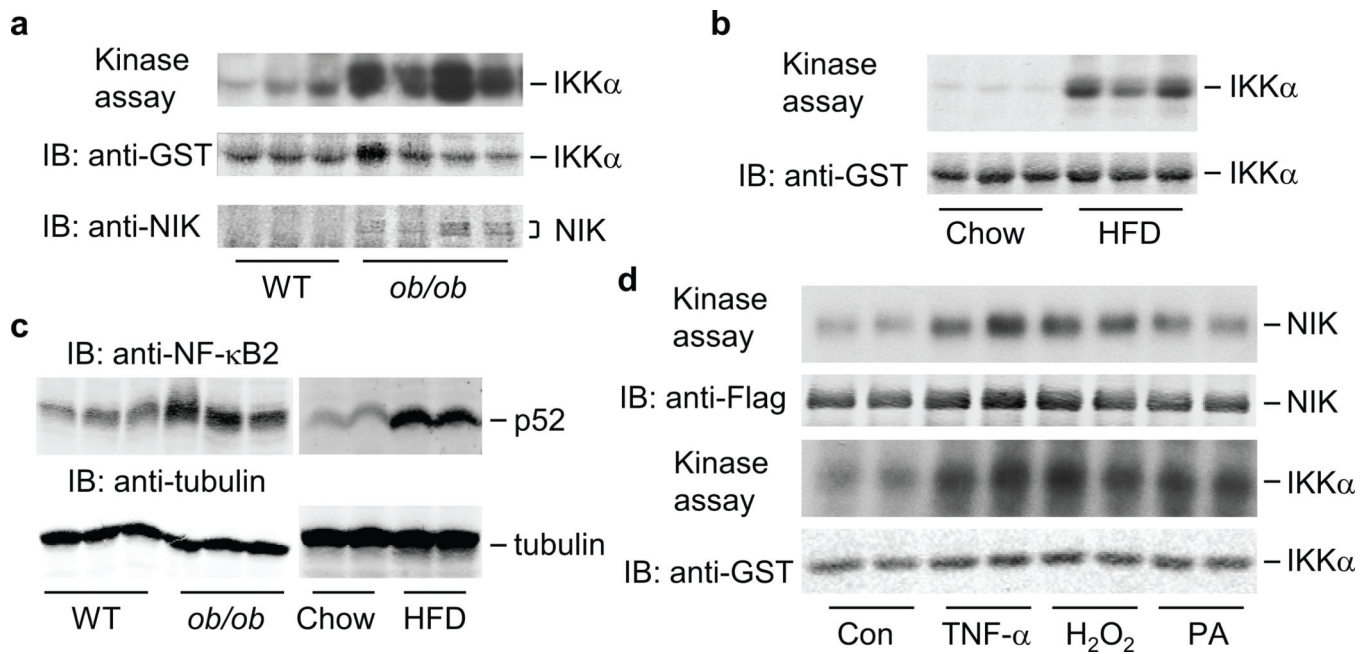
Acknowledgements

We thank Haoran Su, Zhiqin Li, Chaojun Duan, and Ms Suqing Wang for assistance and discussion. We thank Robert Schreiber (Washington University School of Medicine, St. Louis, MO) for providing NIK KO mice and Klaus Rajewsky (Immune Disease Institute, Harvard Medical School, Boston, MA 02115) for providing STOP-NIK mice. Generation of NIK KO mice was supported by Amgen Inc., Thousand Oaks, CA. This study was supported by grants DK 065122 and DK073601 from the US National Institutes of Health and by research award 1-09-RA-156 from the American Diabetes Association. This work utilized the cores supported by the Michigan Diabetes Research and Training Center (funded by NIH 5P60 DK20572), the University of Michigan's Cancer Center (funded by NIH 5 P30 CA46592), the University of Michigan Nathan Shock Center (funded by NIH P30AG013283), and the University of Michigan Gut Peptide Research Center (funded by NIH DK34933).

References

- Hotamisligil GS. Inflammation and metabolic disorders. *Nature*. 2006; 444:860–867. [PubMed: 17167474]
- Shoelson SE, Goldfine AB. Getting away from glucose: fanning the flames of obesity-induced inflammation. *Nat Med*. 2009; 15:373–374. [PubMed: 19350009]
- Arkan MC, et al. IKK-beta links inflammation to obesity-induced insulin resistance. *Nat Med*. 2005; 11:191–198. [PubMed: 15685170]
- Cai D, et al. Local and systemic insulin resistance resulting from hepatic activation of IKK-beta and NF-kappaB. *Nat Med*. 2005; 11:183–190. [PubMed: 15685173]
- Yuan M, et al. Reversal of obesity- and diet-induced insulin resistance with salicylates or targeted disruption of Ikkbeta. *Science*. 2001; 293:1673–1677. [PubMed: 11533494]
- Unger RH, Cherrington AD. Glucagonocentric restructuring of diabetes: a pathophysiologic and therapeutic makeover. *J Clin Invest*. 2012; 122:4–12. [PubMed: 22214853]
- Jiang G, Zhang BB. Glucagon and regulation of glucose metabolism. *Am J Physiol Endocrinol Metab*. 2003; 284:E671–E678. [PubMed: 12626323]
- Denroche HC, et al. Leptin therapy reverses hyperglycemia in mice with streptozotocin-induced diabetes, independent of hepatic leptin signaling. *Diabetes*. 2011; 60:1414–1423. [PubMed: 21464443]
- Yu X, Park BH, Wang MY, Wang ZV, Unger RH. Making insulin-deficient type 1 diabetic rodents thrive without insulin. *Proc Natl Acad Sci U S A*. 2008; 105:14070–14075. [PubMed: 18779578]
- Lee Y, Wang MY, Du XQ, Charron MJ, Unger RH. Glucagon receptor knockout prevents insulin-deficient type 1 diabetes in mice. *Diabetes*. 2011; 60:391–397. [PubMed: 21270251]
- Cummings BP, et al. Subcutaneous administration of leptin normalizes fasting plasma glucose in obese type 2 diabetic UCD-T2DM rats. *Proc Natl Acad Sci U S A*. 2011; 108:14670–14675. [PubMed: 21873226]
- Maruyama H, Hisatomi A, Orci L, Grodsky GM, Unger RH. Insulin within islets is a physiologic glucagon release inhibitor. *J Clin Invest*. 1984; 74:2296–2299. [PubMed: 6392344]
- Thu YM, Richmond A. NF-kappaB inducing kinase: a key regulator in the immune system and in cancer. *Cytokine Growth Factor Rev*. 2010; 21:213–226. [PubMed: 20685151]
- Sun SC. Non-canonical NF-kappaB signaling pathway. *Cell Res*. 2011; 21:71–85. [PubMed: 21173796]
- Yin L, et al. Defective lymphotoxin-beta receptor-induced NF-kappaB transcriptional activity in NIK-deficient mice. *Science*. 2001; 291:2162–2165. [PubMed: 11251123]
- Murray SE, et al. NF-kappaB-inducing kinase plays an essential T cell-intrinsic role in graft-versus-host disease and lethal autoimmunity in mice. *J Clin Invest*. 2011; 121:4775–4786. [PubMed: 22045568]

17. Ling L, Cao Z, Goeddel DV. NF-kappaB-inducing kinase activates IKK-alpha by phosphorylation of Ser-176. *Proc Natl Acad Sci U S A*. 1998; 95:3792–3797. [PubMed: 9520446]
18. Xiao G, Fong A, Sun SC. Induction of p100 processing by NF-kappaB-inducing kinase involves docking IkappaB kinase alpha (IKKalpha) to p100 and IKKalpha-mediated phosphorylation. *J Biol Chem*. 2004; 279:30099–30105. [PubMed: 15140882]
19. Xiao G, Harhaj EW, Sun SC. NF-kappaB-inducing kinase regulates the processing of NF-kappaB2 p100. *Mol Cell*. 2001; 7:401–409. [PubMed: 11239468]
20. Malinin NL, Boldin MP, Kovalenko AV, Wallach D. MAP3K-related kinase involved in NF-kappaB induction by TNF, CD95 and IL-1. *Nature*. 1997; 385:540–544. [PubMed: 9020361]
21. Ninomiya-Tsuji J, et al. The kinase TAK1 can activate the NIK-I kappaB as well as the MAP kinase cascade in the IL-1 signalling pathway. *Nature*. 1999; 398:252–256. [PubMed: 10094049]
22. Sasaki Y, et al. NIK overexpression amplifies, whereas ablation of its TRAF3-binding domain replaces BAFF:BAFF-R-mediated survival signals in B cells. *Proc Natl Acad Sci U S A*. 2008; 105:10883–10888. [PubMed: 18663224]
23. Herzig S, et al. CREB regulates hepatic gluconeogenesis through the coactivator PGC-1. *Nature*. 2001; 413:179–183. [PubMed: 11557984]
24. Zhou XY, et al. Insulin regulation of hepatic gluconeogenesis through phosphorylation of CREB-binding protein. *Nat Med*. 2004; 10:633–637. [PubMed: 15146178]
25. Koo SH, et al. The CREB coactivator TORC2 is a key regulator of fasting glucose metabolism. *Nature*. 2005; 437:1109–1111. [PubMed: 16148943]
26. He L, et al. Metformin and Insulin Suppress Hepatic Gluconeogenesis through Phosphorylation of CREB Binding Protein. *Cell*. 2009; 137:635–646. [PubMed: 19450513]
27. Yoon JC, et al. Control of hepatic gluconeogenesis through the transcriptional coactivator PGC-1. *Nature*. 2001; 413:131–138. [PubMed: 11557972]
28. Liao G, Zhang M, Harhaj EW, Sun SC. Regulation of the NF-kappaB-inducing kinase by tumor necrosis factor receptor-associated factor 3-induced degradation. *J Biol Chem*. 2004; 279:26243–26250. [PubMed: 15084608]
29. Vallabhapurapu S, et al. Nonredundant and complementary functions of TRAF2 and TRAF3 in a ubiquitination cascade that activates NIK-dependent alternative NF-kappaB signaling. *Nat Immunol*. 2008; 9:1364–1370. [PubMed: 18997792]
30. Zarnegar BJ, et al. Noncanonical NF-kappaB activation requires coordinated assembly of a regulatory complex of the adaptors cIAP1, cIAP2, TRAF2 and TRAF3 and the kinase NIK. *Nat Immunol*. 2008; 9:1371–1378. [PubMed: 18997794]
31. Duan C, Yang H, White MF, Rui L. Disruption of the SH2-B gene causes age-dependent insulin resistance and glucose intolerance. *Mol Cell Biol*. 2004; 24:7435–7443. [PubMed: 15314154]
32. Aoki K, et al. Dehydroepiandrosterone suppresses the elevated hepatic glucose-6-phosphatase and fructose-1,6-bisphosphatase activities in C57BL/Ksj-db/db mice: comparison with troglitazone. *Diabetes*. 1999; 48:1579–1585. [PubMed: 10426376]
33. Ren D, et al. Neuronal SH2B1 is essential for controlling energy and glucose homeostasis. *J Clin Invest*. 2007; 117:397–406. [PubMed: 17235396]
34. Zhou Y, Jiang L, Rui L. Identification of MUP1 as a regulator for glucose and lipid metabolism in mice. *J Biol Chem*. 2009; 284:11152–11159. [PubMed: 19258313]
35. Huang W, Dedousis N, Bhatt BA, O'Doherty RM. Impaired Activation of Phosphatidylinositol 3-Kinase by Leptin Is a Novel Mechanism of Hepatic Leptin Resistance in Diet-induced Obesity. *J Biol Chem*. 2004; 279:21695–21700. [PubMed: 14993225]
36. Cho KW, Zhou Y, Sheng L, Rui L. Lipocalin-13 Regulates Glucose Metabolism by both Insulin-Dependent and Insulin-Independent Mechanisms. *Mol Cell Biol*. 2011; 31:450–457. [PubMed: 21135134]
37. Sheng L, Cho KW, Zhou Y, Shen H, Rui L. Lipocalin 13 protein protects against hepatic steatosis by both inhibiting lipogenesis and stimulating fatty acid beta-oxidation. *J Biol Chem*. 2011; 286:38128–38135. [PubMed: 21908604]

**Figure 1.**

NIK is overactivated in the livers of mice with obesity. **(a)** NIK in liver extracts was immunoprecipitated with antibody to NIK and subjected to *in vitro* kinase assays. The blots were subsequently immunoblotted (IB) with antibody to GST and NIK. **(b)** Males (7 weeks) were fed a normal chow diet or an HFD for 6 weeks. NIK in liver extracts was immunopurified with antibody to NIK and subjected to *in vitro* kinase assays. **(c)** Liver extracts were immunoblotted with antibody to NF- κ B2 or Tubulin. **(d)** Primary hepatocytes were infected with Flag-tagged NIK adenoviruses. Sixteen hours after infection, cells were treated for 2 h with a vehicle (Con) or TNF- α (10 ng ml⁻¹), H₂O₂ (100 nM) or PA (100 μ M). NIK was immunoprecipitated with antibody to Flag and subjected to *in vitro* kinase assays. The blots were immunoblotted with antibody to Flag and GST.

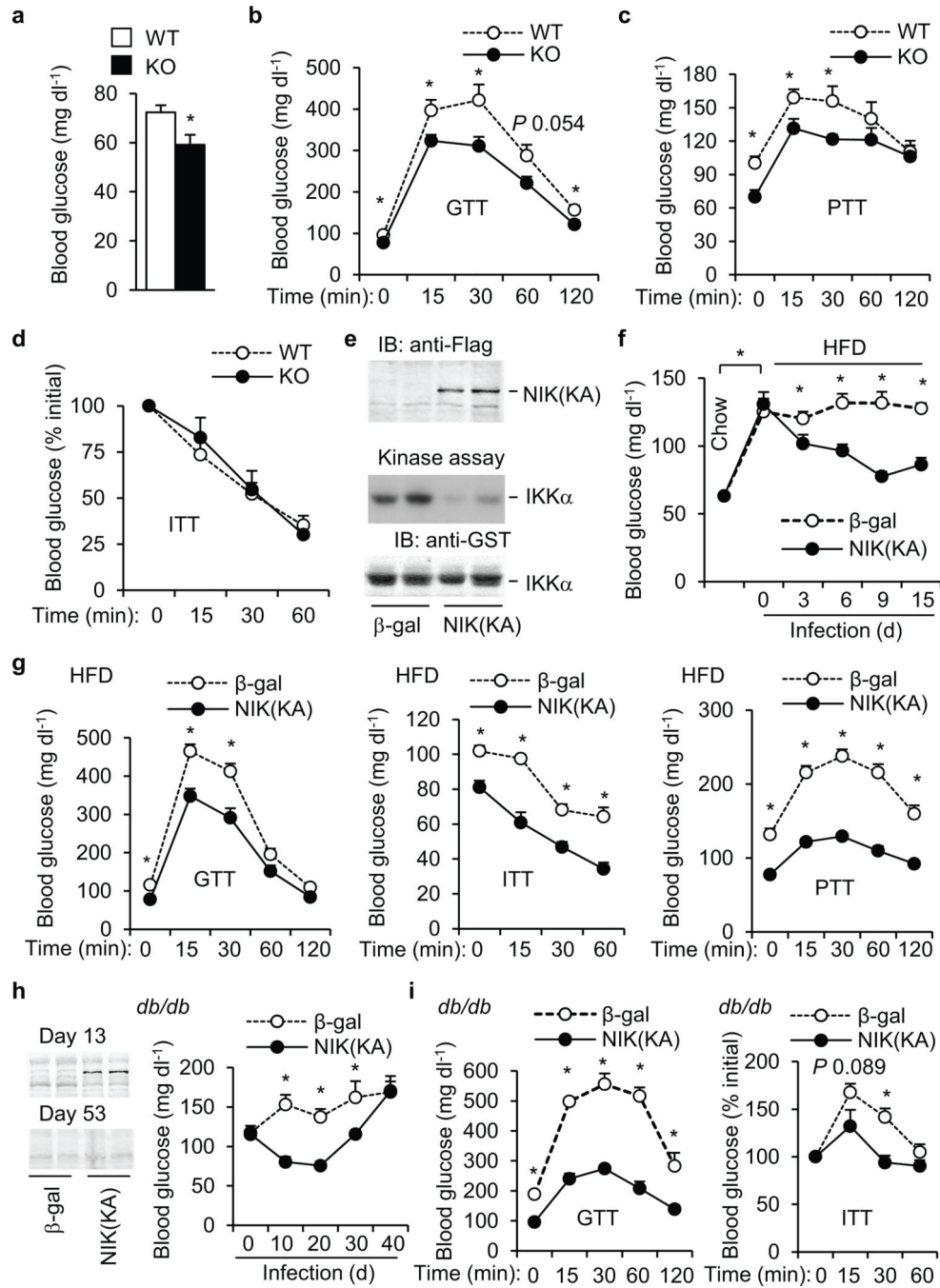


Figure 2. Inhibition of NIK in the liver decreases hyperglycemia and glucose intolerance in mice with obesity. **(a–d)** WT and KO males were fed a normal chow diet. **(a)** Fasting blood glucose. WT: $n=12$, KO: $n=16$, age: 7–8 weeks. **(b)** GTT. WT: $n=8$, KO: $n=11$, age: 8 weeks. **(c)** PTT. WT: $n=8$, KO: $n=11$, age: 8–9 weeks. **(d)** ITT. WT: $n=9$, KO: $n=10$, age: 8 weeks. **(e)** Mice were infected with β -gal or Flag-tagged NIK(KA) adenoviruses for 15 days. Liver extracts were immunoblotted with antibody to Flag. Liver NIK was also immunopurified with antibody to NIK and subjected to *in vitro* kinase assays. **(f–g)** C57BL/6 males (7

weeks) were fed an HFD for 12 weeks and then infected with β -gal or NIK(KA) adenoviruses. (f) Overnight fasting blood glucose. (g) GTT, ITT, and PTT were performed 11, 13, and 9 days after infection, respectively. β -gal: $n=9-10$; NIK(KA): $n=10$. (h-i) *db/db* males (8 weeks) were infected with β -gal ($n=8$) or NIK(KA) ($n=9$) adenoviruses. (h) Left: Liver extracts were immunoblotted with antibody to Flag 13 and 53 days after infection. Right: Overnight fasting blood glucose. (i) GTT (glucose: 0.8 g kg^{-1} body weight) and ITT (insulin: 2.5 U kg^{-1} body weight) were performed 10 and 8 days after infection, respectively. $*P < 0.05$.

Author Manuscript

Author Manuscript

Author Manuscript

Author Manuscript

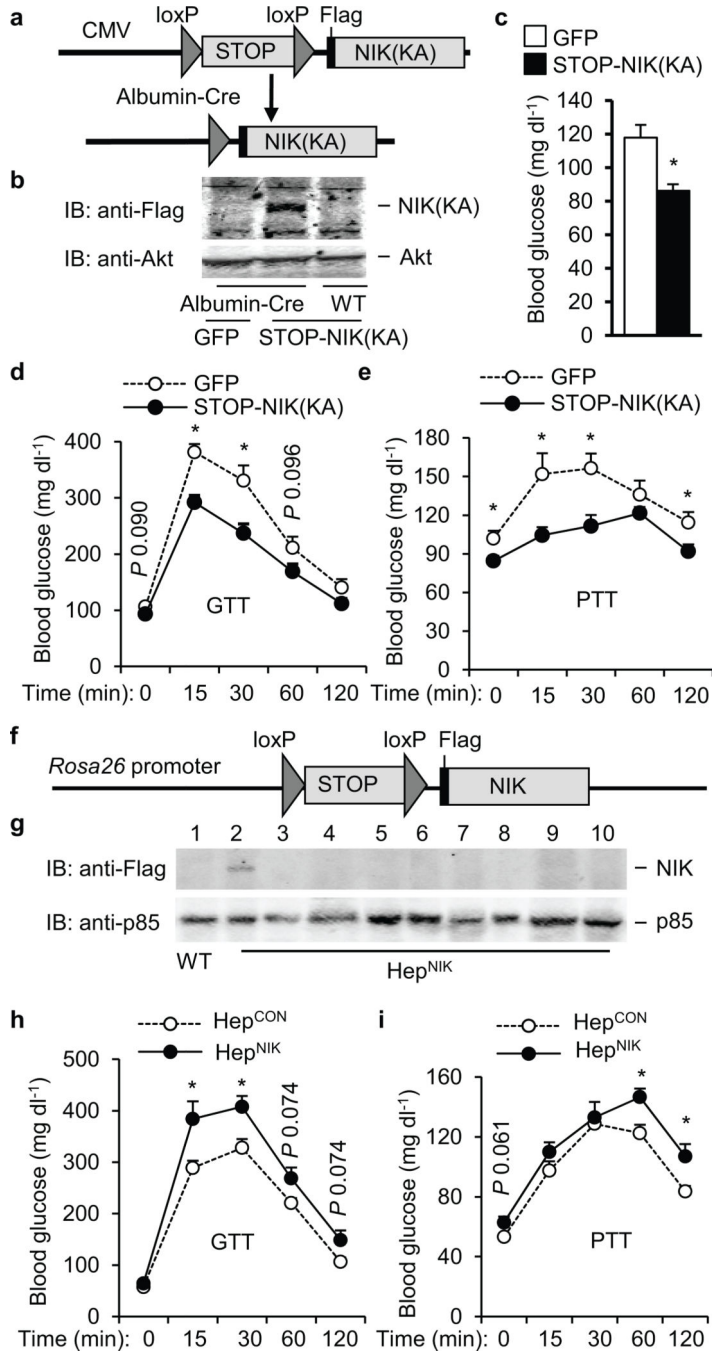
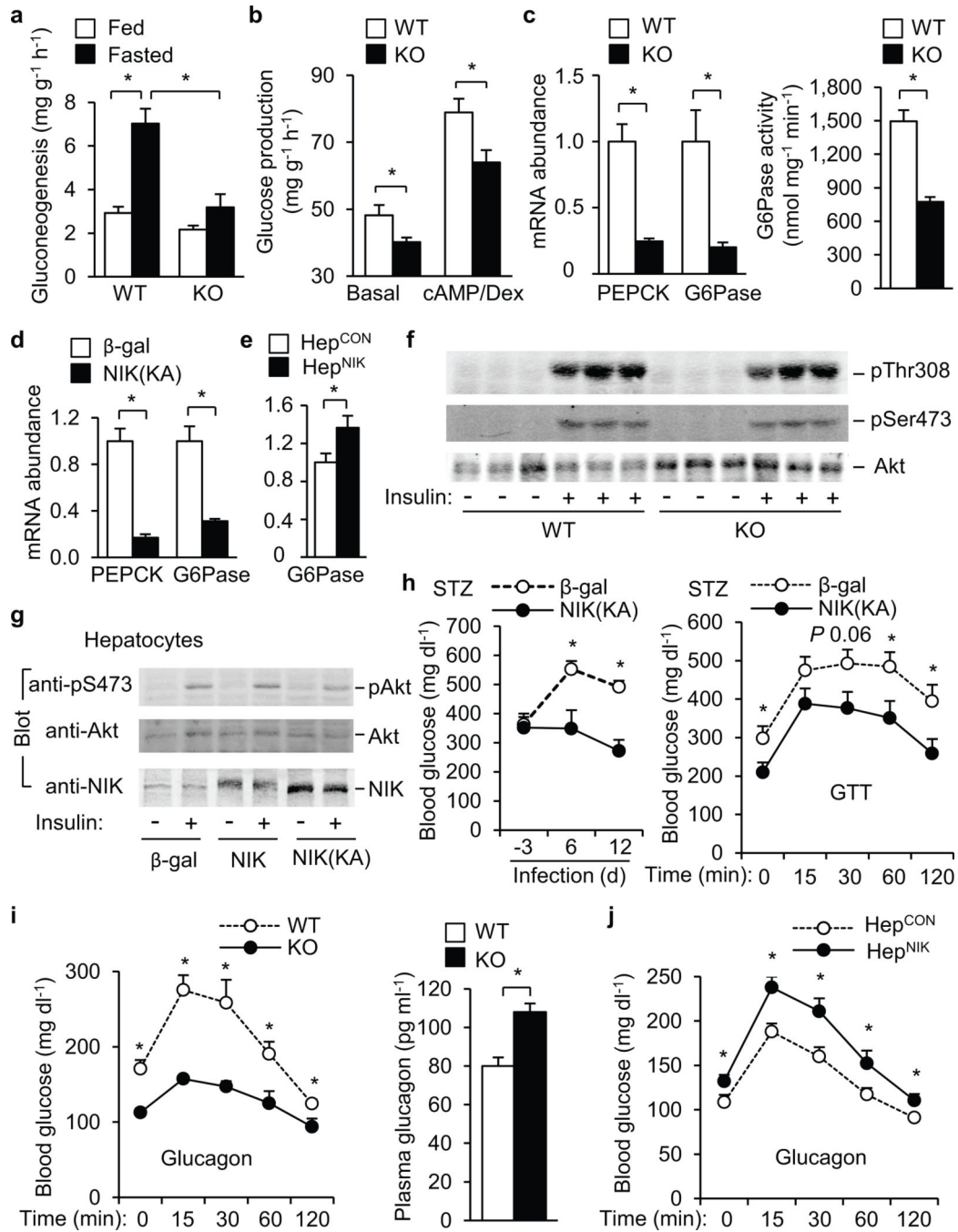


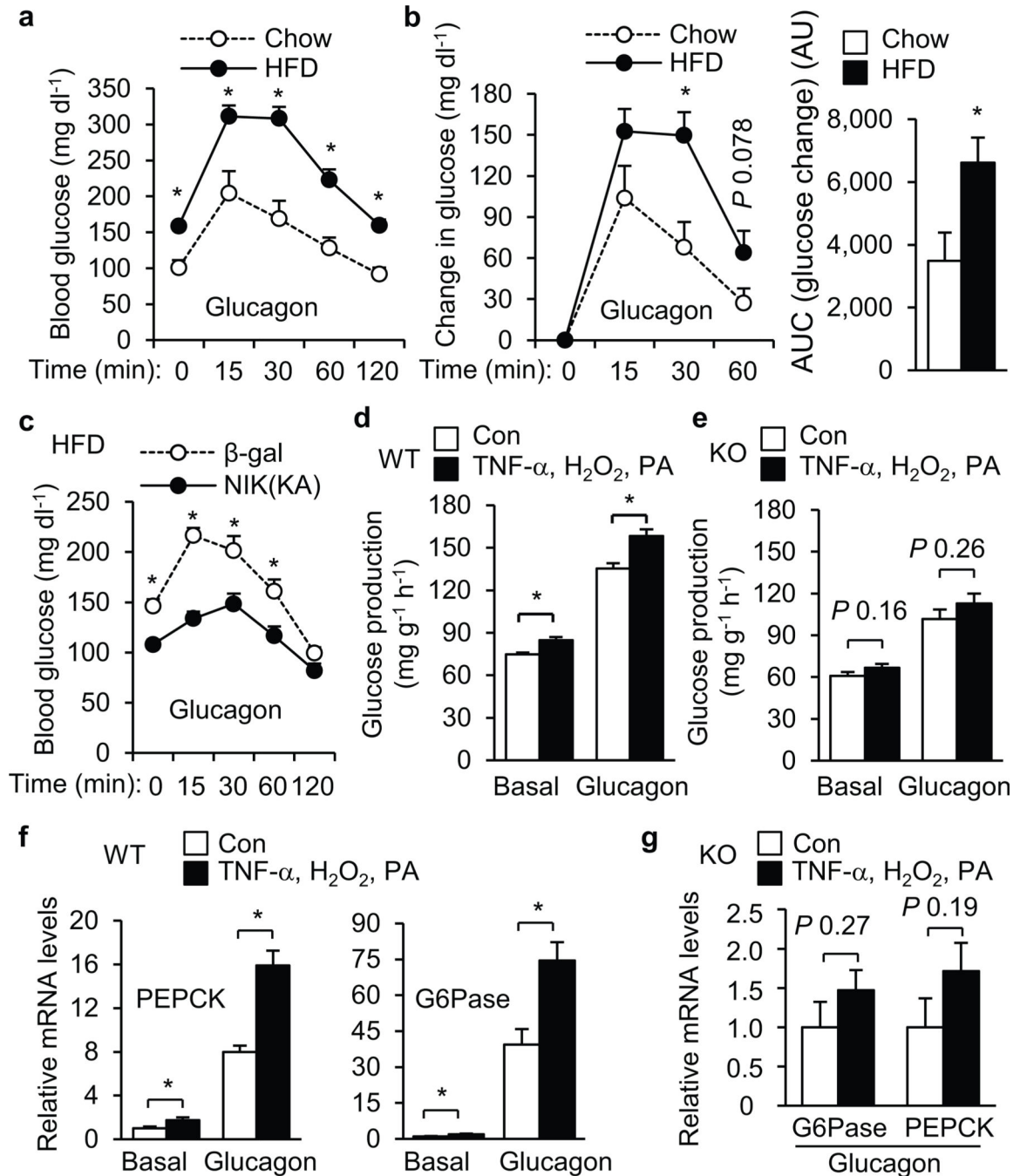
Figure 3. Hepatocyte NIK regulates blood glucose levels and HGP. **(a)** A schematic representation of STOP-NIK(KA) adenoviral vectors. **(b)** WT and albumin-Cre^{+/-} mice were infected with STOP-NIK(KA) or GFP adenoviruses. Liver extracts were immunoblotted with antibody to Flag or Akt 13 days after infection. **(c–e)** Albumin-Cre^{+/-} males (8 weeks) were fed an HFD for 10 weeks and then infected with GFP (*n*=11) or STOP-NIK(KA) (*n*=11) adenoviruses. **(c)** Overnight fasting blood glucose 14 days after infection. **(d)** GTT 7 days after infection. **(e)** PTT 12 days after infection. **(f)** A schematic representation of STOP-NIK targeting

vectors. **(g)** Tissue extracts were prepared from Hep^{CON} (genotype: *STOP-NIK^{+/+}/Cre^{-/-}*) and Hep^{NIK} (genotype: *STOP-NIK^{+/+}/Cre^{+/-}*) males (5 weeks) and immunoblotted with antibody to Flag or p85. Lanes 1–2: liver, 3: pancreas, 4: muscle, 5: brain, 6: white fat, 7: brown fat, 8: spleen, 9: kidney, 10: heart. **(h–i)** Hep^{CON} (genotype: *STOP-NIK^{+/-}/CRE^{-/-}*, *n*=10) and Hep^{NIK} (genotype: *STOP-NIK^{+/-}/CRE^{+/-}*, *n*=7) males were fed a normal chow diet for 15 weeks. **(h)** GTT. **(i)** PTT. **P* < 0.05.

**Figure 4.**

NIK promotes glucagon stimulation of glucose production. (a) Gluconeogenesis in isolated livers ($n=5$). (b) Glucose production in primary hepatocytes treated with DB-cAMP (10 μ M) and dexamethasone (100 nM) ($n=8$). (c) Relative mRNA abundance of hepatic *PEPCK* and *G6Pase* in WT ($n=9$) and KO ($n=9$) males (9 weeks) and hepatic *G6Pase* activity in WT ($n=7$) and KO ($n=6$) males (19 weeks). (d–e) Relative mRNA abundance of hepatic *PEPCK* and *G6Pase* in *db/db* males infected with β -gal ($n=5$) or NIK(KA) adenoviruses ($n=6$) for 13 days (d) and in Hep^{CON} ($n=10$) and Hep^{NIK} males ($n=7$) (e). (f) WT and KO mice (9 weeks)

were fasted overnight and stimulated with insulin (2 U kg^{-1} body weight) for 5 min. Liver extracts were immunoblotted with antibody to phospho-Akt or Akt. **(g)** Primary hepatocytes were infected with β -gal, NIK, or NIK(KA) adenoviruses, and stimulated with 100 nM insulin for 10 min 48 h after infection. Cell extracts were immunoblotted with antibody to pSer473, Akt, or NIK. **(h)** C57BL/6 males (8 weeks) were injected intraperitoneally with STZ and infected with β -gal ($n=6$) or NIK(KA) ($n=6$) adenoviruses 5 days after injection. Randomly-fed blood glucose and GTT (glucose: 0.25 g kg^{-1} body weight; 9 days after infection) were examined. **(i)** Glucagon tolerance tests in WT ($n=5$) and KO ($n=7$) males (14 weeks) and overnight fasting plasma glucagon levels in WT ($n=11$) and KO ($n=8$) males (14 weeks). **(j)** Glucagon tolerance tests in Hep^{CON} ($n=10$) and Hep^{NIK} ($n=9$) males (14 weeks). * $P < 0.05$.

**Figure 5.**

NIK mediates HFD and TNF- α , H₂O₂ and PA-induced enhancement of glucagon action. (a) C57BL/6 males (8 weeks) were fed a normal chow diet ($n=5$) or HFD ($n=9$) for 6 weeks, fasted for 5 h, and intraperitoneally injected with glucagon (10 $\mu\text{g kg}^{-1}$ body weight). Blood glucose was monitored. (b) Glucagon-stimulated increase in blood glucose (left) and the areas under the curves (AUC) (right) were calculated. AU: arbitrary units. (c) C57BL/6 males (7 weeks) were fed an HFD for 6 weeks and infected with β -gal ($n=10$) or NIK(KA) adenoviruses ($n=10$). Seven days after infection, mice were subjected to glucagon (10 μg

kg⁻¹ body weight) injection experiments. **(d–e)** Primary hepatocytes were prepared from WT **(d)** and KO **(e)** mice and pretreated with vehicles (Con) or TNF- α , H₂O₂ and PA for 4 h, and then treated with glucagon (50 nM) for additional 4 h. Glucose production was measured and normalized to total protein levels. **(f–g)** WT **(f)** and KO **(g)** primary hepatocytes were treated with TNF- α , H₂O₂ and PA for 4 h and then with glucagon for additional 2 h. The expression of *PEPCK* and *G6Pase* was measured by qPCR and normalized to β -actin expression. * $P < 0.05$.

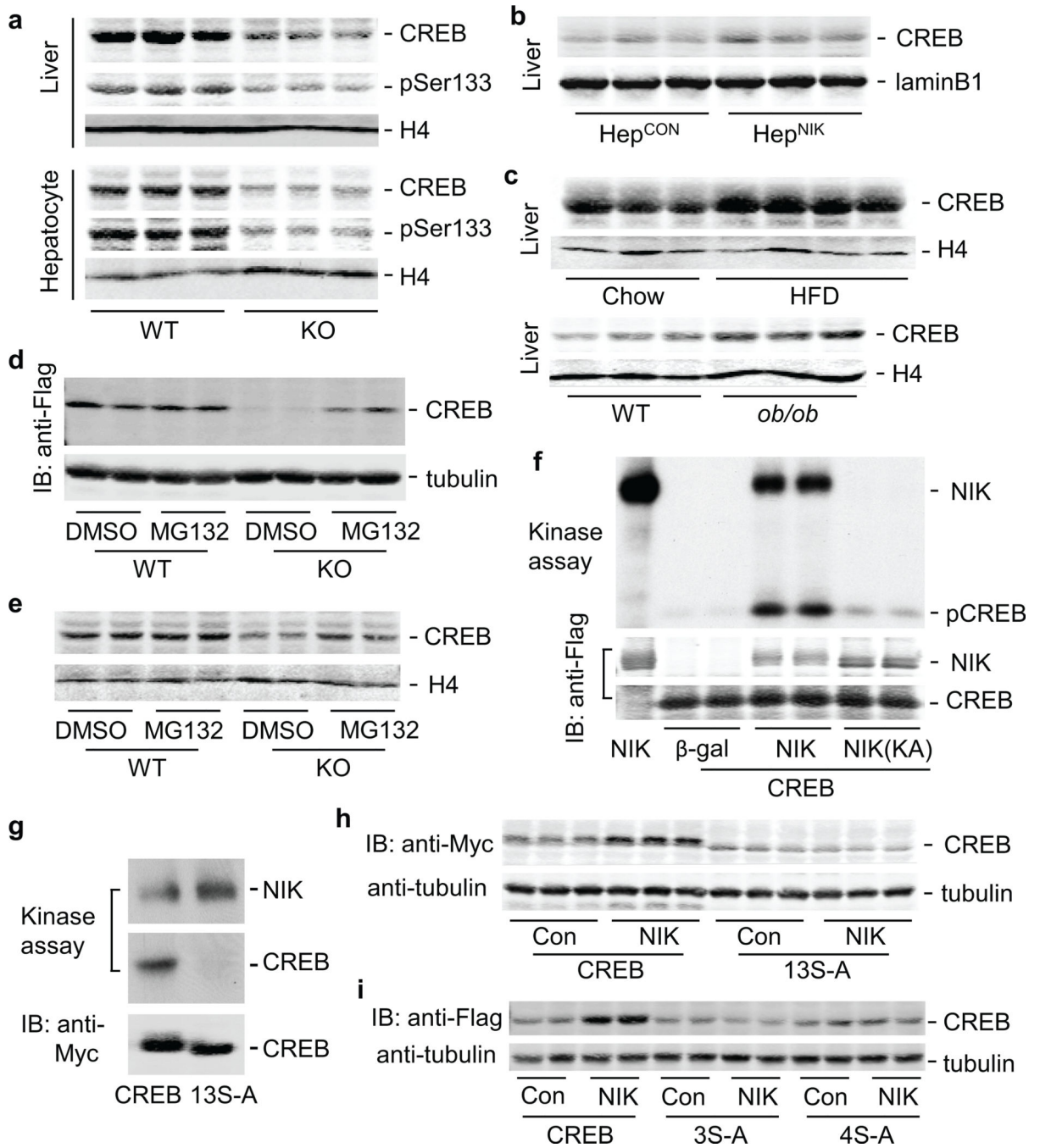


Figure 6. NIK phosphorylates CREB and increases CREB stability. **(a)** Nuclear extracts were immunoblotted with antibody to CREB, phospho-CREB (pSer133), and H4 (histone 4). **(b)** Liver nuclear extracts were prepared from Hep^{CON} and Hep^{NIK} males (17–8 weeks) and immunoblotted with antibody to CREB or LaminB1. **(c)** Liver nuclear extracts were prepared from WT males fed a normal chow diet or HFD for 6 weeks or from WT and *ob/ob* males (13 weeks), and immunoblotted with antibody to CREB or H4. **(d)** Primary hepatocytes were infected with Flag-tagged CREB adenoviruses for 16 h, and treated with a

DMSO vehicle or MG132 (50 μ M) for 9 h. Cell extracts were immunoblotted with antibody to Flag or Tubulin. **(e)** Primary hepatocytes were treated with DMSO or MG132. Nuclear extracts were immunoblotted with antibody to CREB or H4. **(f)** Primary hepatocytes were co-infected with Flag-tagged CREB and Flag-tagged NIK, NIK(KA), or β -gal adenoviruses. Cell extracts were immunoprecipitated with antibody to Flag and subjected to *in vitro* kinase assays. The blots were immunoblotted with antibody to Flag. **(g)** Myc-tagged CREB and 13S-A were immunopurified and subjected to *in vitro* NIK kinase assays. **(h)** HepG2 cells were co-transfected with NIK and Myc-tagged CREB or 13S-A plasmids. Cell extracts were prepared 48 h after transfection and immunoblotted with antibody to Myc or Tubulin. **(i)** HepG2 cells were co-transfected with NIK and Flag-tagged CREB, 3S-A, or 4S-A plasmids. Cell extracts were immunoblotted with antibody to Flag or Tubulin.

Author Manuscript

Author Manuscript

Author Manuscript

Author Manuscript